Acta Med. Okayama, 2016
Vol. 70, No. 1, pp. 13–24

Acta Medica Okayama
http://escholarship.lib.okayama-u.ac.jp/amo/

Original Article

The Function of β2-glycoprotein I in Angiogenesis and Its *in Vivo* Distribution in Tumor Xenografts

Arum Tri Wahyuningsih[a], Lianhua Shen[b,c], Kazuko Kobayashi[b], Takanori Sasaki[b], Fumiaki Takenaka[b], Takahisa Hanada[b], Masaru Akehi[b], Akiya Akahoshi[b], Eiichi Ozeki[c], Eiji Ando[d], and Eiji Matsuura[a,b]*

[a]Department of Cell Chemistry and [b]Collaborative Research Center (OMIC), Okayama University Graduate School of Medicine, Dentistry and Pharmaceutical Sciences, Okayama 700–8558, Japan, [c]Technology Research Laboratory, Shimadzu Corporation, Kyoto 619–0237, Japan, and [d]Life Science Business Department, Shimadzu Corporation, Kyoto 604–8511, Japan

Intact β2-glycoprotein I (iβ2GPI) is a glycoprotein that regulates coagulation and fibrinolysis. Nicked β2GPI (nβ2GPI) possesses an angiogenic property at a relatively low concentration, and an anti-angiogenic property at a high concentration. Here we investigated the functions of iβ2GPI and nβ2GPI in vascular endothelial growth factor (VEGF)-A-induced endothelial cell proliferation and tube formation. We used noninvasive PET imaging to analyze the *in vivo* distribution of intravenously injected β2GPI variants in tumor lesions in mice. iβ2GPI was incubated with plasmin to obtain nβ2GPI, and its N-terminal sequence was analyzed. nβ2GPI had at least one other cleavage site upstream of the β2GPI's domain V, whereas the former plasmin-cleavage site locates between K^{317} and T^{318}. Both of intact and nicked β2GPI significantly inhibited the VEGF-A-induced cell proliferation and the tube formation of human umbilical vein endothelial cells (HUVECs). PET imaging visualized considerably distributed intensities of all tested β2GPI variants in tumor lesions of pancreatic tumor cell-xenografts. These results indicate that β2GPI may be physiologically and pathophysiologically important in the regulation of not only coagulation and fibrinolysis, but also angiogenesis.

Key words: β2-glycoprotein I (β2GPI), angiogenesis, vascular endothelial growth factor-A (VEGF-A), positron emission tomography (PET) imaging

β2-Glycoprotein I (β2GPI) is a 44-kDa phospholipid-binding protein that is present in normal human plasma at a concentration of approx. 200 μg/ml (4 μM) [1]. Intact β2GPI (iβ2GPI) has 5 characteristic domains (DI, DII, DIII, DIV, and DV), as so-called "Sushi" domains. These domains structurally resemble each other, although DV has a hydrophobic extra C-terminal loop with a positively charged lysine/arginine cluster that can interact with negatively charged substances, such as phospholipids, heparin, DNA, platelets, oxidized low-density lipoprotein and apoptotic bodies [2, 3]. In the 1990s, Matsuura and his colleagues reported that the anticardiolipin antibody (aCL) associated with clinical thrombosis required a cofactor to bind the cardiolipin, and the cofactor was identified as β2GPI, which plays a role as a natural anticoagulant or pro-coagulant due to its ability to bind to negatively charged phospholipids [4–6]. As a major antigenic target for antiphospho-

Received August 7, 2015; accepted September 14, 2015.
*Corresponding author. Phone:+81-86-235-7402; Fax:+81-86-235-7404
E-mail:eijimatu@md.okayama-u.ac.jp (E. Matsuura)

Conflict of Interest Disclosures: No potential conflict of interest relevant to this article was reported.

lipid antibodies, β2GPI's pathophysiological roles in the fields of coagulation, fibrinolysis, and angiogenesis have frequently been investigated.

In thrombosis, β2GPI plays a role as an anticoagulant regulator. Anti-coagulant activity is triggered by the binding of β2GPI to phosphatidylserine as a cofactor for particular reactions in the coagulation cascade that inhibit the generation of factor Xa from factor X and the generation of prothrombin to thrombin. These inhibition capabilities were blocked by antiphospholipid antibodies (anti-β2GPI), resulting in the promotion of thrombosis in antiphospholipid syndrome (APS) [7]. In fibrinolysis, domain V (DV) of β2GPI is frequently cleaved by plasmin between Lys-317 and Thr-318 to become a nicked form of β2GPI (nβ2GPI), which cannot bind to phospholipids [8, 9]. nβ2GPI is known as a physiologic inhibitor of fibrinolysis by specifically binding to plasminogen and suppressing the plasmin generation [10].

Angiogenesis plays a role in both physiologic and pathologic states such as reproduction and embryogenesis, inflammation and tumorigenesis, and thrombosis and wound repair [11, 12]. Vascular endothelial growth factor (VEGF) signaling is required for the full execution of angiogenesis [13]. The major member of the VEGF family, VEGF-A, has the molecular weight 42-46 kDa and serves as a dimer [14]. VEGF-A has higher-affinity binding to VEGF receptor (VEGFR)-1 than VEGFR-2, but the level of phosphorylation of VEGFR-2 in response to VEGF-A is stronger than that of VEGFR-1 [15].

The role of β2GPI's biological functions in angiogenesis were determined as anti-angiogenic, as reported by Yu *et al.* [16], who also showed that β2GPI significantly inhibited VEGF- and basic fibroblast growth factor (bFGF)-induced angiogenesis and that the inhibition activity may be mediated through its DI binding. nβ2GPI has also been described as a potent anti-angiogenic and anti-tumor molecule of potential therapeutic significance [17, 18]. In contrast, at lower concentrations nβ2GPI has a significant binding capability to angiostatin 4.5 (AS4.5; plasmin autoproteolysis) that attenuates the anti-angiogenic functions of AS4.5, resulting in the promotion of angiogenesis [17].

Treatments using targeted therapies were recently applied to tumors. As angiogenesis is the key to a tumor's autonomy, the ability to monitor the angiogenesis process *in vivo* will contribute to the management of such interventions. Positron emission topography (PET), which could be used for this purpose [19], is a noninvasive molecular imaging modality that can characterize biological processes in tissues and organs, and it is used to measure the *in vivo* biodistribution of imaging agents labeled with positron-emitting radionuclides [20].

In the present study, we evaluated the ability of iβ2GPI and nβ2GPI to inhibit VEGF-A-induced cell proliferation and tube formation, using human umbilical vein endothelial cells (HUVECs). We speculated that β2GPI might have physiologically and/or pathophysiologically important roles in the regulation of not only coagulation and fibrinolysis, but also angiogenesis. We also suspected that β2GPI can distribute into tumor lesions, which may prove beneficial to the development of diagnostic and targeted therapies.

Materials and Methods

β2GPI variants. iβ2GPI was prepared from fresh normal plasma as described [21] and nβ2GPI was prepared by incubating iβ2GPI with plasmin. In brief, to obtain nβ2GPI, recombinant human plasmin from Wako Pure Chemical Industries (Osaka, Japan) was fixed to Affi-Gel 10 gels (Bio-Rad, Osaka, Japan) and incubated with iβ2GPI at 37℃ for 16 h, and then the supernatant was recovered. We verified the cleavage by sodium dodecylsulfate-polyacrylamide gel electrophoresis (SDS-PAGE) on 4-20% a Tris-HCl gel under non-reducing/reducing conditions, and then we identified the bands by N-terminal sequencing with the use of a PPSQ-33B protein sequencer (Shimadzu, Kyoto, Japan).

N-terminal sequence and MALDI-TOF MS analysis. The plasmin-cleavage site of iβ2GPI was identified by its N-terminal sequence. Briefly, we separated purified intact/nicked β2GPI by SDS-PAGE and electroblotted the protein bands onto Immobilon® PVDF transfer membranes (0.2 μm pore size, Merck Millipore, Cork, Ireland). The membranes were stained with Coomassie Brilliant Blue, and the bands of iβ2GPI and nβ2GPI were cut out and then destained with 60% methanol. Sequencing was analyzed using the protein sequencer.

We performed AXIMA® Performance matrix assisted laser desorption ionization time-of-flight mass

spectrometry (MALDI-TOF MS; Shimadzu) to confirm the purity and to detect the molecular weight of intact/nicked β2GPI. Sinapinic acid (SA) purchased from Shimadzu was used as the matrix. The MALDI-TOF MS was performed using a positive ion source in reflectron mode. The data were collected using Launch Pad 2.8 software used to control the spectrometer (Shimadzu). The mass-to-charge ratio (m/z) was obtained by external calibration using bovine serum albumin (BSA) and bovine insulin (Sigma Aldrich, St. Louis, MO, USA).

Cell culture. HUVECs were obtained from Kurabo Industries (Osaka, Japan) and cultured in a moisturized chamber at 37℃ with 5% CO_2, using the cell-culture medium HuMedia-EG2 (Kurabo) supplemented with a final concentration of 2% fetal calf serum (FCS), 10 ng/ml human epidermal growth factor (hEGF), 5 ng/ml human fibroblast growth factor (hFGF), 10 μg/ml heparin, 1.34 μg/ml hydrocortisone, 50 ng/ml amphotericin B, and 50 μg/ml gentamicin. HUVECs from passages 2 to 6 were used in the following experiments.

Cell proliferation assay. To observe the effects of each β2GPI variant on the proliferation of HUVECs, we performed a cell proliferation assay. The experiment was done using HuMedia-EG2 medium with hEGF reduced to a final concentration of 5 ng/ml. First, 5×10^3 HUVECs in 100 μl of medium were seeded into the wells of a 96-well microtiter plate, cultured for 24 h and then serum-starved for another 3 h. Different concentrations of iβ2GPI and nβ2GPI with/without 2.5 ng/ml of human recombinant VEGF-A (Kurabo) were added to the medium. After a 72-h incubation at 37℃, 10 μl of Cell Counting Kit-8 (Dojindo, Kumamoto, Japan) was added to the wells and the cells were incubated for another 3.5 h at 37℃. The optical density (OD) at 450 nm was then measured. Triplicate assays were performed 3 times.

In vitro tube formation. A 96-well microtiter plate was coated with 50 μl of Cultrex® Basement Membrane Extract (BME) Reduced Growth Factor gels (Trevigen, Gaithersburg, MD, USA) and solidified for 60 min at 37℃. HUVECs (1×10^4 per well) were seeded onto the surface of the gel and cultured in HuMedia-EG2 medium without heparin and with hEGF reduced to a final concentration of 5 ng/ml. Assays were performed according to the manufacturer's instructions (Trevigen) in the absence or presence of VEGF-A (5 ng/ml) and intact/nicked β2GPI at the final concentration of 0.05 to 1 μM. Sulforaphan was added to the culture as a potent angiogenesis inhibitor. Tube length formation was monitored over a 6-h period and photographed with a fluorescence microscopic imaging system (model IX71, Olympus, Tokyo, Japan; 4× magnification). The image analysis of the tube length formation was carried out using Image J Angiogenesis Analyzer, v1.49q software.

Enzyme-linked immunosorbent assay (ELISA) for human VEGF-A. We cultured and maintained the pancreatic carcinoma cell lines CFPAC-1 & MIA PaCa-2 (ATCC, Manassas, VA, USA) using Iscove's Modified Dulbecco's Medium (IMDM; Gibco/Life Technologies, Tokyo, Japan), PANC-1 (ATCC) using Dulbecco's Modified Eagle Medium (DMEM; Gibco/Life Technologies) and BxPC-3 (ATCC) using Roswell Park Memonal lnstitute (RPMI)-1640 (Gibco/Life Technologies) added with 10% FBS and 1% of Penicillin-Streptomycin Mixed Solution (Nacalai Tesque, Kyoto, Japan). Each of the 4 cell lines (1×10^6 cells) was seeded into 10-cm dishes containing the complete medium. The cultured media were collected after the cell growth reached 80-90% confluence. We performed an ELISA for human VEGF-A with collected cultured media from the pancreatic carcinoma cell lines as specified by the manufacturer's instructions using a human VEGF-A kit from R&D Systems (Minneapolis, MN, USA).

Inoculating tumor cells to mice. All animal experiments were supervised under Okayama University guidelines and in agreement with the University's Animal Care and Use Committee (OKU-2013098). The human pancreatic cancer cell line CFPAC-1 (CRL-1918TM, ATCC) derived from liver metastasis was cultured at 37℃ with 5% CO_2, using IMDM as described above containing 10% FBS and 1% Penicillin-Streptomycin Mixed Solution. The cultured cancer cells were harvested, washed, and re-suspended with Matrigel using a 1 : 1 volume ratio before being injected into mice.

Five-week-old male BALB/c nu/nu mice (Charles River, Tokyo, Japan) were inoculated subcutaneously with CFPAC-1 cells (3×10^6 cells) per mouse on the right shoulder. The body weights of the mice and the volumes of the tumors were measured 2 weeks after the inoculation, and the tumor-bearing mice were then prepared for PET imaging.

Conjugation with a chelating agent and radiolabeling of β2GPI variants. One-hundred mM EDTA (3 μl) was added to iβ2GPI and nβ2GPI (1 mg) to complex any free trace metal ion. Both iβ2GPI and nβ2GPI were concentrated into 0.1 M HEPES (pH 8.9) by centrifugation in Amicon Ultra 0.5 10K centrifugal tubes (Merck Milipore, Tokyo, Japan). Conjugation with 2-S-(4-isothiocyanatobenzyl)-1,4,7-triazacyclononane-1,4,7-triacetic acid (*p*-SCN-Bn-NOTA: Macrocyclics, Dallas, TX, USA) was applied to iβ2GPI, iβ2GPI in the presence of dioleoylphosphatidylglycerol (DOPG) and nβ2GPI. To avoid *p*-SCN-Bn-NOTA (NOTA) conjugation at the phospholipid binding region in DV, NOTA was reacted to iβ2GPI in the presence of DOPG. Briefly, DOPG solution in chloroform was dried in a glass tube under N_2, added with 0.1 M HEPES buffer (pH 8.9) and then sonicated. Next, iβ2GPI was mixed with DOPG micelle solutions with a 1 : 1 volume ratio and incubated for 30 min at room temperature to make iβ2GPI-DOPG complex.

Conjugation to the NOTA chelator was achieved as described with slight modification [22, 23]. NOTA was dissolved with dimethyl sulfoxide (DMSO; Sigma-Aldrich) to make 22.4 mg/ml solution by vortex and sonication. An 80-fold molar concentration of NOTA-DMSO solution was added into iβ2GPI, the iβ2GPI-DOPG complex solutions and nβ2GPI, and then conjugation was allowed to proceed at 37℃ for 1 h with gentle mixing. All reaction mixtures were then fractionated using PD-10 columns (Sephadex G-25 M, GE Healthcare, Buckinghamshire, UK) with phosphate-buffered saline (PBS) to separate the NOTA-conjugated variants (NOTA-iβ2GPI, NOTA-DOPG-iβ2GPI and NOTA-nβ2GPI) from free NOTA. The DOPG in the NOTA-DOPG-iβ2GPI was then delipidated with n-butanol. We named the delipidated protein as NOTA-iβ2GPI (masked).

For radiolabeling, Copper-64 (^{64}Cu) (239-269 MBq) diluted in 5 mg/ml gentisic acid saline and 0.1 M phosphate buffer (pH 5.5) was added to 0.2 mg of NOTA-iβ2GPI, 0.2 mg of NOTA-iβ2GPI (masked), or 0.165 mg of NOTA-conjugated nβ2GPI (NOTA-nβ2GPI), respectively. All reaction mixtures were incubated at 37℃ for 10 min, and then we used thin layer chromatography and autoradiography (TLC-ARG) to confirm the radiolabeling efficiency. Briefly, each sample was spotted on a silica gel plate (at the original position) developed using 50 mM EDTA (pH 8.0). The NOTA-β2GPI variants-bound ^{64}Cu radioactivity stayed at the origin and unbound ^{64}Cu went to the upper part of the chromatogram. The reaction mixtures were then supplemented with 10% 0.1 M EDTA (pH 7.0) and centrifuged in Amicon Ultra 0.5 10K centrifugal tubes to eliminate the free ^{64}Cu.

ELISA for antibody binding. To measure the antibody binding ability to negatively charged lipids of iβ2GPI, NOTA-iβ2GPI, NOTA-iβ2GPI (masked) and nβ2GPI, we performed an ELISA, as previously described [24]. Fifty μg/ml of cardiolipin was immobilized onto the wells of a 96-well microtiter plate (Immulon IB, Thermo Scientific, Rochester, NY, USA) and allowed to dry. The wells were then blocked with PBS containing 0.2% BSA for 1 h at room temperature and washed 3 times with 0.05% Tween-20 in PBS. Serial dilutions of the sample solutions were added to the wells and incubated for 1 h. After 3 washes, the wells were treated with 1 μg/ml of Cof-20 antibody for 1 h. The wells were then washed, and antibody binding against domain III of β2GPI was detected by 30-min incubation with peroxidase-labeled anti-mouse IgG (Life Technologies, Tokyo, Japan). After 3 washes, color was developed by adding 100 μl of TMB-US substrate (Moss, Pasadena, MD, USA) to the wells. To stop the reaction, 100 μl of 2N H_2SO_4 was applied, and then the OD values were measured at 450 nm with a microplate reader (Bio-Rad 550, Hercules, CA, USA).

PET imaging and tissue biodistribution. Each mouse bearing a CFPAC-1 tumor was anesthetized by isoflurane inhalation and intravenously injected with approx. 20 MBq/20 μg of ^{64}Cu-NOTA-iβ2GPI (n = 3), 26 MBq/20 μg of ^{64}Cu-NOTA-iβ2GPI (masked) (n = 3), or 15 MBq/21 μg of ^{64}Cu-NOTA-nβ2GPI (n = 3). We conducted emission scans for 10 min (at 0 h), 30 min (at 24 h) and 60 min (at 48 h) using a small-animal PET scanner (Clairvivo PET, Shimadzu), and the images were reconstructed using the 3D-DRAMA method. At the end of the final PET scans at 48 h post-injection, all mice were sacrificed for biodistribution studies.

In addition, separate groups of mice (n = 3 each) were administered ^{64}Cu-NOTA-iβ2GPI (20 MBq), ^{64}Cu-NOTA-iβ2GPI (masked) (26 MBq), or ^{64}Cu-NOTA-nβ2GPI (approx. 2 MBq) and sacrificed 24 h post-injection for biodistribution studies. The tumors

and major organs of the mice were collected and weighed, and we measured the radioactivity of the organs with a gamma-counter (AccuFLEX γ7001, Hitachi Aloka Medical, Tokyo, Japan). The biodistribution data are expressed as the percentage of the injected dose per gram of tissues (% ID/g).

Statistical analysis. The statistical significance of the data was evaluated by Student's *t*-test. Probability values < 0.05 were considered significant.

Results

Purification and characterization of nβ2GPI. iβ2GPI showed a single band by SDS-PAGE analysis under reducing conditions. The SDS-PAGE analysis of nβ2GPI confirmed that iβ2GPI was cleaved and the resulting band showed an interval with the band of iβ2GPI (Fig. 1A). N-Terminal sequencing identified that iβ2GPI was cleaved by plasmin under non-reducing conditions, and N-terminal sequences were confirmed ($G^{1}RT \times PKPDDLPF$, $T^{318}DASDVK$). In that experiment, a novel N-terminal sequence (another cleavage site sensitive to plasmin at the upstream in DV rather than T^{318}) was also identified (data not shown). Proteolytic cleavage seems to be reasonable to explain the MALDI-TOF MS size difference (*i.e.*, the average molecular weights of iβ2GPI and nβ2GPI determined by MALDI-TOF MS were 44 kDa and 38 kDa, respectively) as shown in Fig. 1B. We are now testing these results using a set of recombinant mutant proteins of β2GPI; we will publish those data elsewhere.

Effects of the β2GPI variants on the VEGF-A-dependent proliferation of HUVECs. The growth of the HUVECs treated with VEGF-A at concentrations from 1.25 to 10 ng/ml increased dose-dependently (Fig. 2A). The VEGF-A at 2.5–10 ng/ml significantly increased the growth of the HUVECs. To observe the inhibitory effect of β2GPI on VEGF-A-induced cell growth, we incubated HUVECs with intact/nicked β2GPI in the presence of 2.5 ng/ml of VEGF-A. As shown in Fig. 2B, intact/nicked β2GPI decreased the VEGF-A-induced growth of the HUVECs in a dose-dependent manner. Nicked β2GPI significantly suppressed the HUVECs' growth at the concentrations of 0.125, 0.5 and 1 μM, whereas iβ2GPI significantly suppressed the VEGF-A-induced growth of the cells at the lowest to the highest concentrations (0.063–1 μM). These results indicate the inhibitory role of iβ2GPI and nβ2GPI on VEGF-A-induced HUVECs cell proliferation.

Effects of the β2GPI variants on the VEGF-A-dependent tube formation of HUVECs. To observe the tube formation of HUVECs and to evalu-

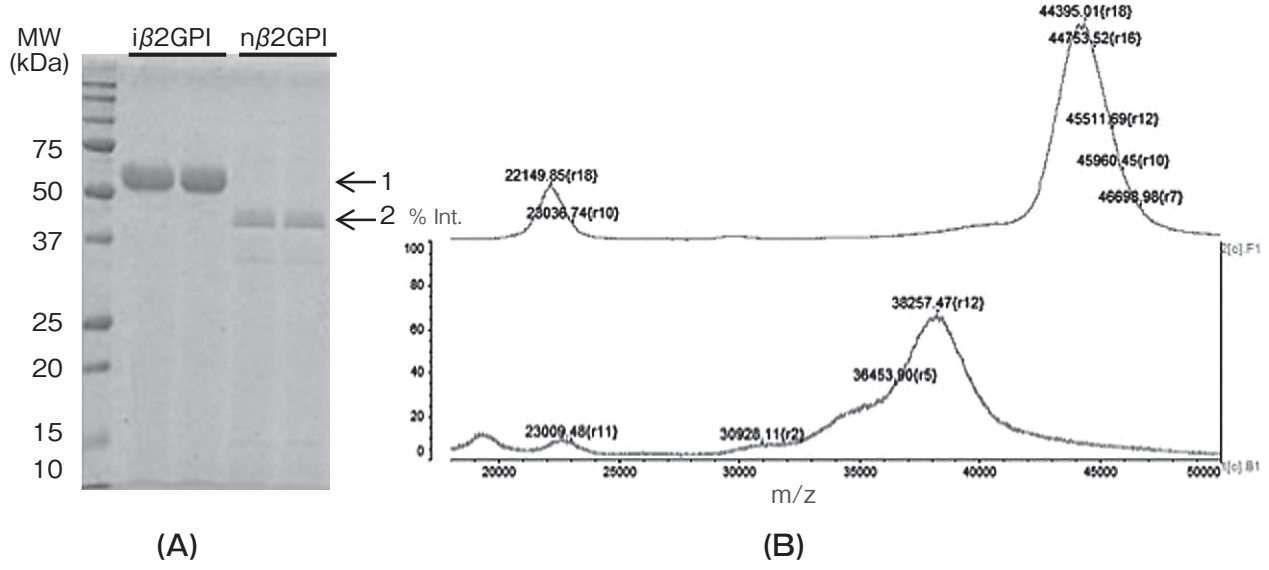

Fig. 1 Purification of nicked β2GPI. (A) 1, iβ2GPI and 2, iβ2GPI cleaved by plasmin (nβ2GPI) showed a clear band on SDS-PAGE Tris-HCl gradient gel (4–20%) under reducing conditions. (B) The molecular weights of iβ2GPI (top graph) and nβ2GPI (bottom) determined by MALDI-TOF MS were 44 kDa and 38 kDa, respectively.

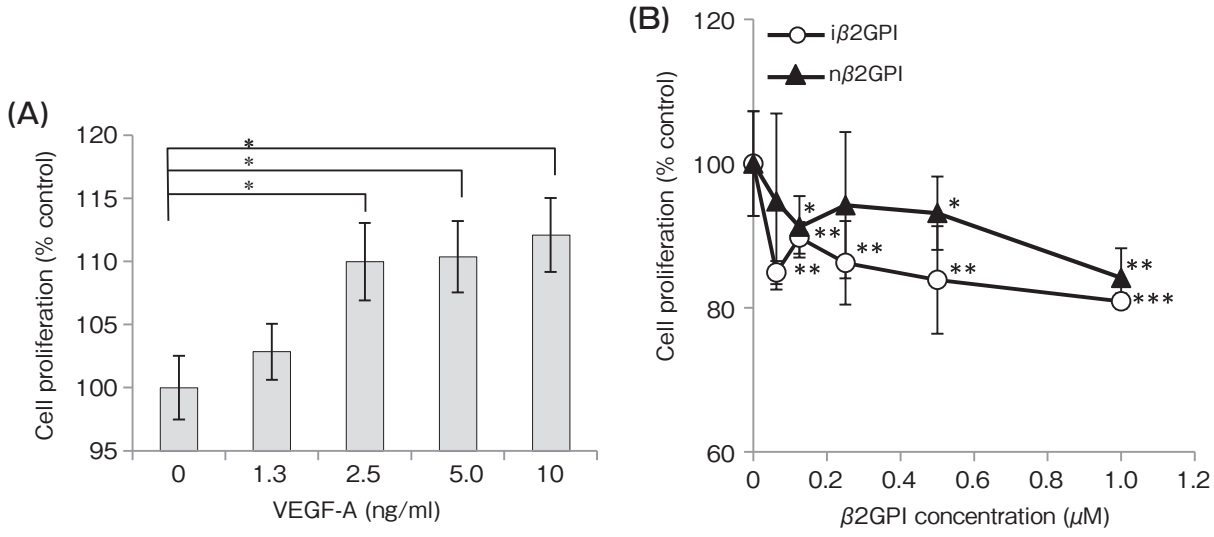

Fig. 2 Potent inhibitory effects of β2GPI variants on the VEGF-A-dependent proliferation of HUVECs. (**A**) HUVECs were treated with the denoted concentrations of VEGF-A for 72 h. (**B**) The effect of iβ2GPI (open circles) and nβ2GPI (solid triangles) at various concentrations with 2.5 ng/ml VEGF-A on the HUVECs' growth. The cells' survival was determined with a Cell Counting Kit-8. Values are expressed as the percentage of the control group (VEGF-alone; set as 100%). $^{*}p < 0.05$, $^{**}p < 0.01$, $^{***}p < 0.001$ vs. VEGF-alone (control).

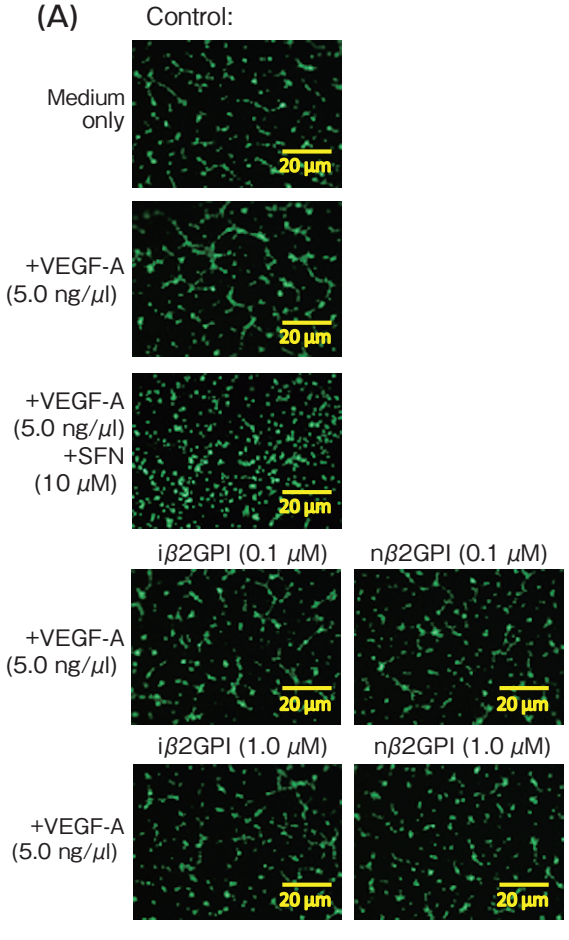

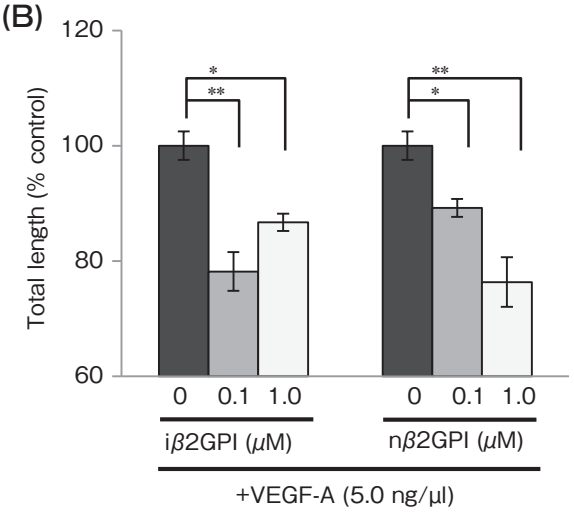

Fig. 3 Effects of β2GPI variants on the VEGF-A-dependent tube formation of HUVECs. The VEGF-A-dependent tube formation of HUVECs was evaluated using serial concentrations. Sulforaphan (SFN) (10 μM) was used as a negative control and VEGF-A (5 ng/ml) as a positive control. (**A**) HUVECs were visualized by fluorescence microscopy with serial concentrations of intact and nicked of β2GPI (original magnification × 4). VEGF-A (5 ng/ml) was added to all protein concentrations. (**B**) Tube length formation was quantified using ImageJ Angiogenesis Analyzer, ver. 1.49q. The data (total length) were plotted onto the bar graphs: intact β2GPI and nicked β2GPI. Values are expressed as the percentage of the VEGF-alone control group set as 100%. $^{*}p < 0.05$, $^{**}p < 0.01$ vs. VEGF-alone.

ate the inhibition of angiogenesis by each protein, we conducted *in vitro* angiogenesis assays. The treatment of the cells with iβ2GPI and nβ2GPI resulted in the suppression of VEGF-A-stimulated tube formation. Fig. 3A shows examples of the tube formation of untreated and/or treated HUVECs by fluorescence microscopy. In this assay, higher concentrations of iβ2GPI and nβ2GPI suppressed the tube length formation. Significant effects on VEGF-A-dependent tube formation obtained by iβ2GPI and nβ2GPI were observed (Fig. 3B).

Expression of VEGF-A by the four pancreatic carcinoma cell lines. VEGF-A was detected in all four of the human pancreatic carcinoma cell lines used in this study (Fig. 4). Compared to the other cell lines, the CFPAC-1 cells grew relatively rapidly and secreted the largest amount of VEGF-A in their culture supernatant. We therefore decided to inoculate the mice with CFPAC-1 cells (xenografts) for the PET imaging studies.

Conjugation with NOTA and radiolabeling. NOTA-iβ2GPI, NOTA-iβ2GPI (masked) and NOTA-nβ2GPI were each purified by column chromatography with PD-10, and then the average molecular weights were measured by MALDI-TOF MS. The average number of NOTA molecules per iβ2GPI, iβ2GPI (masked) and nβ2GPI molecules were 3.8, 2.9 and 1.3, respectively. These numbers were determined by dividing the mass difference between each NOTA-β2GPI variants and iβ2GPI or nβ2GPI by the molecular weight of NOTA (559.9 Da). We then determined the binding ability to solid-phase cardiolipin of NOTA-conjugated β2GPI by performing an ELISA to observe the effect of NOTA conjugation. nβ2GPI appeared to be unbound to cardiolipin (Fig. 5A) because the phospholipid binding site was cleaved by plasmin. Fig. 5B shows that the binding of NOTA-iβ2GPI (masked) to cardiolipin was moderate com-

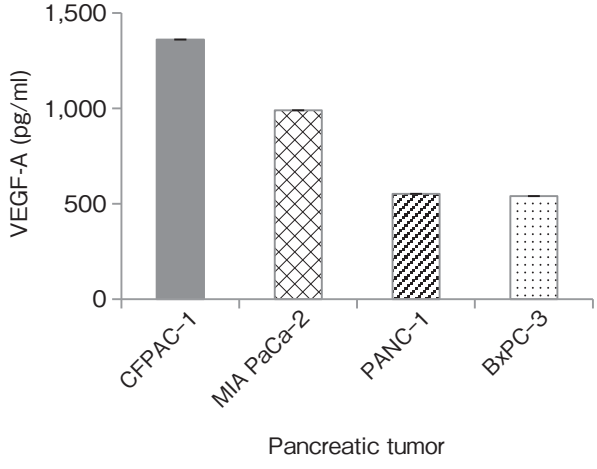

Fig. 4 Human VEGF-A ELISA. Among the four pancreatic tumor cell lines tested, the CFPAC-1 tumor cells secreted the largest amount of VEGF-A as determined by a human VEGF-A ELISA.

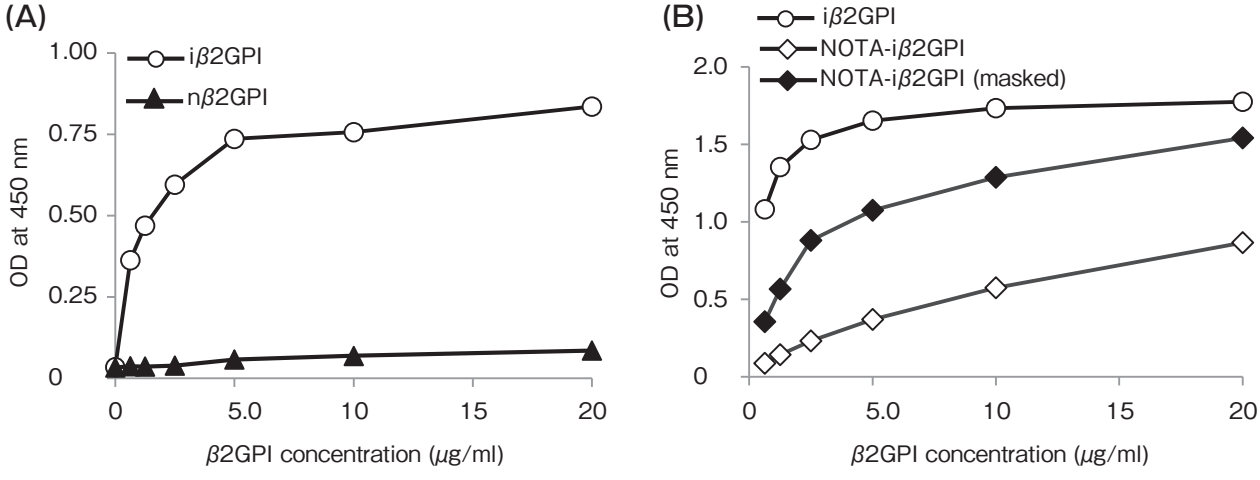

Fig. 5 Binding activity to cardiolipin by ELISA. The binding activity to cardiolipin of (**A**) iβ2GPI (open circles) compared to that of nβ2GPI (solid triangles), and the activities of (**B**) NOTA-iβ2GPI (open diamonds) and NOTA-iβ2GPI (masked) (solid diamonds) compared to that of iβ2GPI (open circles) as determined by ELISA. Cardiolipin was immobilized, and then iβ2GPI and its variants were added to the wells. After incubation with Cof-20, antibody binding was detected with peroxidase-labeled anti-mouse IgG and TMB substrate. The reaction was stopped with 2N H_2SO_4 and the OD was measured at 450 nm.

pared to the original iβ2GPI, whereas the binding of NOTA-iβ2GPI was much lower than that of iβ2GPI. These results indicated that the NOTA molecule was conjugated to lysine residue(s) which are located closely or exactly on the phospholipid binding site of β2GPI in NOTA-iβ2GPI. The results also indicated that the masking of DOPG in NOTA-iβ2GPI (masked) prevented the conjugation of NOTA to the site(s).

The radiolabeling of NOTA-conjugated β2GPI showed radiolabeling efficiency of 96.4%, 97.1% and 88.3% for ^{64}Cu-NOTA-iβ2GPI, ^{64}Cu-NOTA-iβ2GPI (masked) and ^{64}Cu-NOTA-nβ2GPI, respectively. The specific activities of ^{64}Cu-NOTA-iβ2GPI, ^{64}Cu-NOTA-iβ2GPI (masked) and ^{64}Cu-NOTA-nβ2GPI were 0.98, 1.3 and 0.71 MBq/μg at the end of purification, respectively.

PET imaging and biodistribution studies. To observe the *in vivo* distribution of β2GPI and its variants in tumor lesions, we performed the PET studies. PET imaging of ^{64}Cu-NOTA-iβ2GPI, ^{64}Cu-NOTA-iβ2GPI (masked), and ^{64}Cu-NOTA-nβ2GPI was done with tumor-bearing mice at 0, 24 and 48 h post-injection. Fig. 6 shows the resulting PET images. Considerable intensities could be observed in the tumor lesions at 24 and 48 h.

Following the PET imaging studies, all mice were euthanized for biodistribution studies as shown at Fig. 7A, B. The intensity of each probe was greatest in the kidney, the liver and the tumor, in that order. The ratios of tumor to blood and tumor to muscle

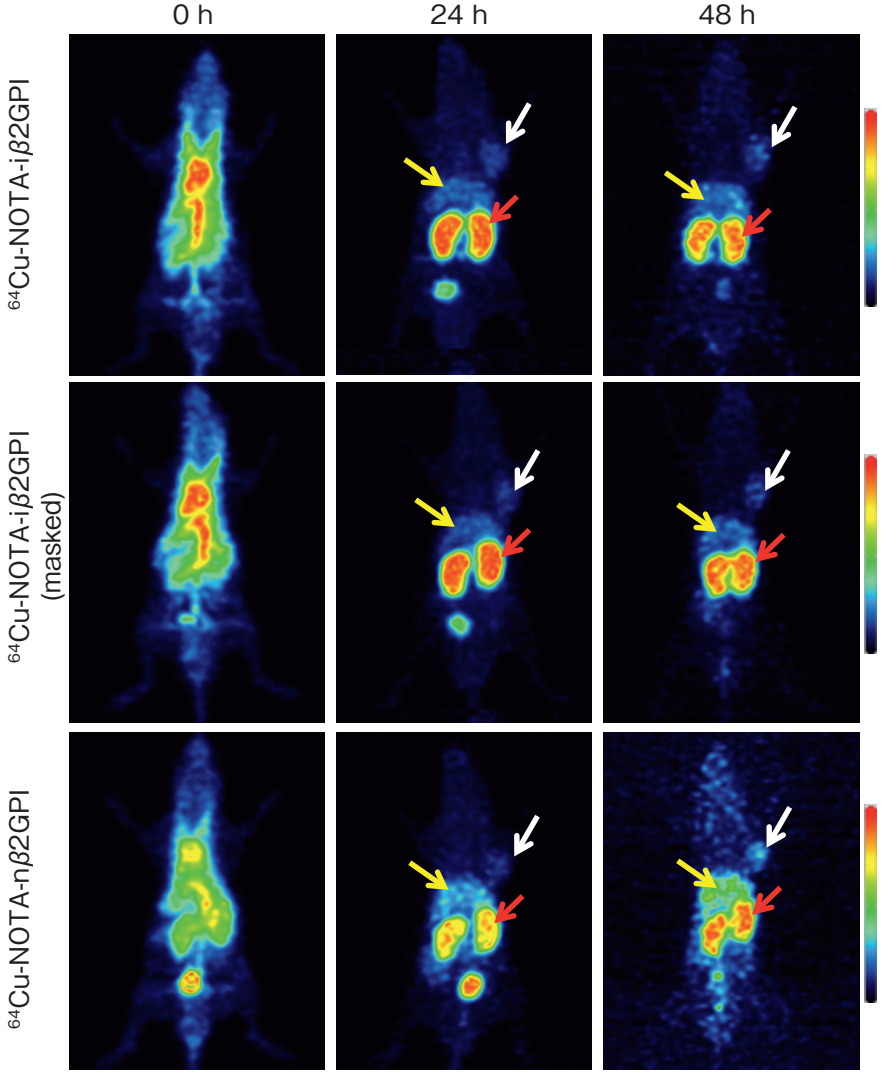

Fig. 6 PET imaging. Representative PET images of the tumor-bearing mice at 0, 24 and 48 h after the injections of β2GPIs-labeled ^{64}Cu. Images show the maximum intensity projections (MIP) of whole bodies. From top to bottom: a mouse injected with ^{64}Cu-NOTA-iβ2GPI, ^{64}Cu-NOTA-iβ2GPI (masked) and ^{64}Cu-NOTA-nβ2GPI. The upper thresholds of PET images were adjusted for visual clarity, as indicated by the scale bars. Considerable intensities were observed in the kidney (red arrow), the liver (yellow arrow) and the tumor (white arrow).

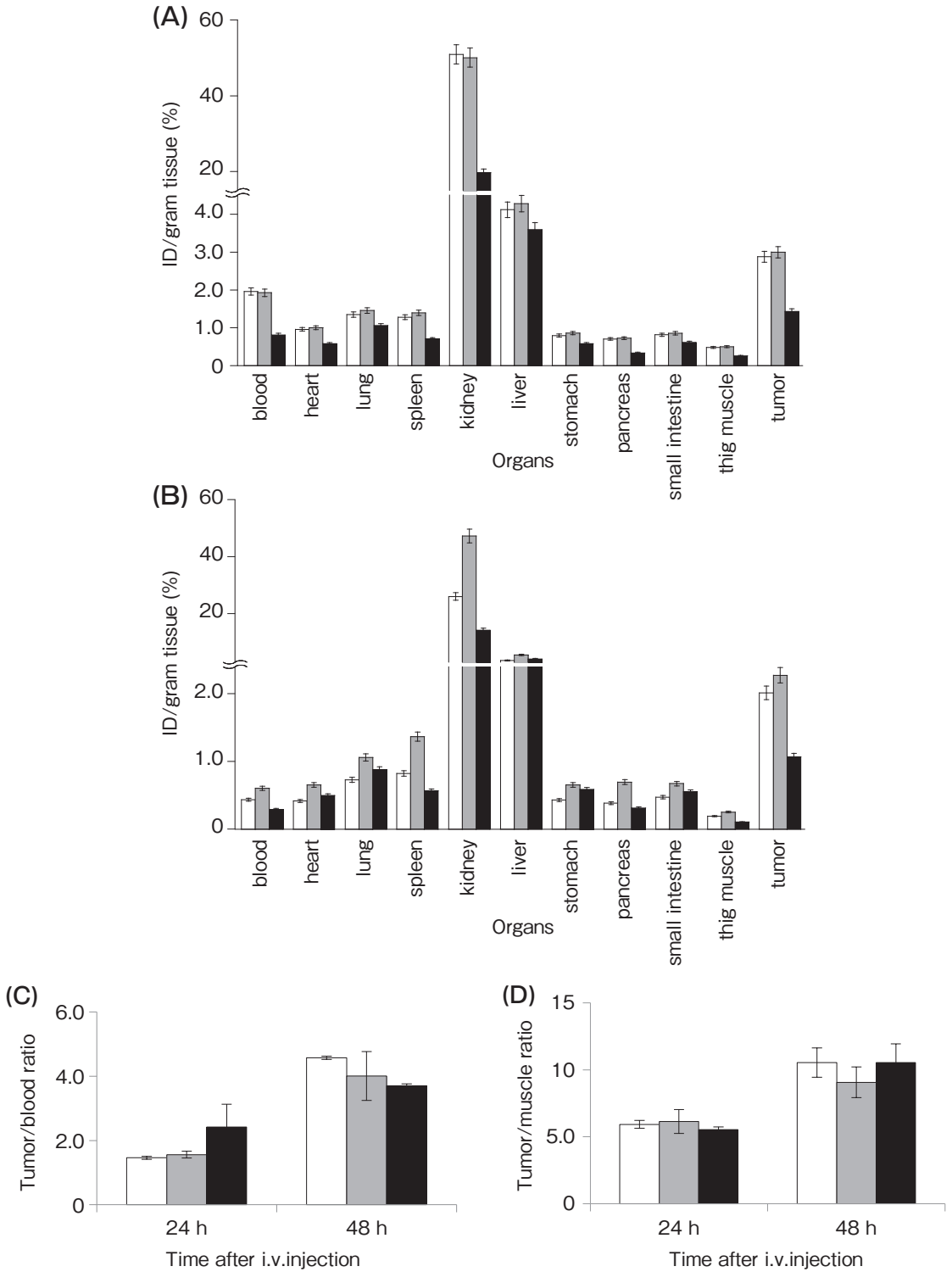

Fig. 7 Biodistribution studies of ^{64}Cu-NOTA-conjugated β2GPI variants. Biodistribution of probes at (**A**) 24 h and (**B**) 48 h in tumor-bearing mice after they were i.v.-injected with ^{64}Cu-NOTA-iβ2GPI (white bars), ^{64}Cu-NOTA-iβ2GPI (masked) (gray bars) or ^{64}Cu-NOTA-nβ2GPI (black bars). The data were calculated as the % of injected dose per gram of tissue (%ID/g). The ratios of tumor to blood (**C**) and tumor to muscle (**D**) at 24 and 48 h post-injection are shown.

(Fig. 7C, D) showed the probes level to attain the tumor region which were normalized by the blood and the muscle.

Discussion

To determine the precise role of β2GPI in angiogenesis－toward the development of therapeutic medication－we performed *in vitro* and *in vivo* experiments using purified iβ2GPI and nβ2GPI. The *in vitro* experiment was conducted because endothelial cells have an essential role in the process of vascular remodeling. HUVECs are commonly employed for physiological and pharmacological investigations; *e.g.*, studies of blood coagulation, angiogenesis and fibrinolysis. We used PET imaging in the present *in vivo* study to investigate the intensity level of β2GPI and its *in vivo* distribution, because PET is noninvasive and is directed to the entire body.

β2GPI was described as the major antigen for aCL, which binds to anionic phospholipids [3–6]. The binding of β2GPI to phospholipid via its C-terminal loop was reported to be significantly reduced by plasmin cleavage between K^{317} and T^{318} [8, 9]. In this study, we are surprised to discover cleavage sites in DV of β2GPI other than the cleavage between K^{317} and T^{318}. Numerous studies [8, 9, 24, 25] have discussed iβ2GPIs' plasmin-cleavage including the cleavage site at K^{317}–T^{318}, but there were few studies regarding the molecular weight difference between iβ2GPI and nβ2GPI based on SDS-PAGE gel results under non-reducing condition.

The present study is the first to use MALDI-TOF MS to confirm the molecular weights of intact/nicked β2GPI, as this is a new approach for both. The MALDI-TOF MS findings clearly showed that the average molecular weight of nβ2GPI (38 kDa) is quite different from that of iβ2GPI (44 kDa), which corresponds to the individual bands of iβ2GPI and nβ2GPI in the SDS-PAGE results. Under reducing conditions, the disulfide (S-S) bonds will be reduced by 2-mercaptoethanol, whereas nβ2GPI showed a much different size compared to iβ2GPI; ＞935 Da larger (from T^{318} to C^{326}). Our results suggest that nβ2GPI has at least one more cleavage site upstream of β2GPI's domain V in which the former plasmin-cleavage site is located between K^{317} and T^{318}. Further studies are needed to explore the roles of nβ2GPI cleavages.

Several studies showed that iβ2GPI and nβ2GPI have angiogenic properties that could suppress tumor growth by blocking the neovascularization [18, 26, 27]. In the present study, we find that iβ2GPI inhibited the VEGF-A-induced cell proliferation and VEGF-A-stimulated tube formation of HUVECs. These results do not contradict those of the Chiu *et al.* [28] report that β2GPI suppressed VEGF-induced endothelial cell growth and migration. Similar results regarding the cell proliferation and tube formation induced by VEGF-A were obtained in the present study by incubating HUVECs with nβ2GPI.

Our results are also in concurrence with those of Sakai *et al.* [18] and Beecken *et al.* [29], who reported inhibitory effects of nβ2GPI on endothelial cell proliferation *in vitro* and vascularization *in vivo*. Based on our findings, we propose that intact/nicked β2GPI may have inhibitor property against VEGF-A-dependent angiogenesis. It is debatable whether β2GPI downregulates the VEGF-A or VEGFR-1/VEGFR-2 directly. Another investigation is required to clarify whether intact/nicked β2GPIs' role in angiogenesis involves direct binding to VEGF-A or VEGFR-1/VEGFR-2.

We used PET imaging with iβ2GPI and nβ2GPI to test the recent results studies indicating that intact and nicked β2GPI possess angiogenic properties that may prove beneficial for the development of therapeutic medicine as an angiogenesis-targeted treatment. The imaging study was necessary to evaluate the distribution of both proteins in tumor-bearing mice. Compared to other pancreatic tumor cells (MIA PaCa-2 and PANC-1), CFPAC-1 cells strongly expressed microRNA-21 (miR-21) which was positively correlated with the expression of mRNA of VEGF [30]. Our present experiment showed that CFPAC-1 cells grew relatively rapidly and secreted the largest amount of VEGF-A among the 4 tumor cell lines examined, and for this reason we inoculated CFPAC-1 cells into mice for the PET imaging. As a chelating agent for ^{64}Cu, we used NOTA. Zhang *et al.* [31] had revealed that NOTA is one of the best chelators for the ^{64}Cu-labeling of proteins, macromolecules or nanomaterials.

We prepared 3 probes to evaluate the intensity of each probe in CFPAC-1 tumors by PET imaging, which are ^{64}Cu-NOTA-iβ2GPI, ^{64}Cu-NOTA-iβ2GPI (masked) and ^{64}Cu-NOTA-nβ2GPI. The binding of

NOTA-iβ2GPI (masked) to cardiolipin indicated that the affinity to the cardiolipin was similar to that of the original iβ2GPI, even after conjugation with NOTA (Fig. 5B). We suspect that these results reflect the ability of NOTA-conjugated β2GPIs to bind cardiolipin. In addition, the masking effect by DOPG at β2GPIs' phospholipid binding site influenced the average number of NOTA-conjugated molecules.

Even though the angiogenesis assay results suggested that iβ2GPI more effectively suppressed the VEGF-A-dependent cell proliferation compared to nβ2GPI, the three probes showed similar kinetic efficiency at 24 and 48 h. In addition, there were no significant differences between them in the PET imaging results. It is possible that iβ2GPI suppressed the HUVEC proliferation as a result of β2GPI expression by the endothelial cells [32].

We observed the considerable intensities of the iβ2GPI variants in the tumor lesions. A possible explanation of this result is that it was caused by the binding of β2GPI to some sort of molecule(s) such as VEGF-A in the tumor lesions. However, we are not able to exclude the possibility that the intensities observed in the tumor lesions led to the abundant circulating blood in the tumors, which have rich neovascular vessels. Further investigation is needed to investigate the several potential binding activities of iβ2GPI and nβ2GPI to other molecules in the tumor lesions, such as annexin II [33], toll-like receptor 2 (TLR2) [34], and other receptors in tumors.

In conclusion, we found that nβ2GPI has at least one other cleavage site upstream of the β2GPI's DV in which the former plasmin-cleavage site between K^{317} and T^{318} is located. Our findings also demonstrated iβ2GPI and nβ2GPI as angiogenesis inhibitors of VEGF-A-induced HUVECs cell proliferation and tube formation. These results indicate that β2GPI may be physiologically and pathophysiologically important in the regulation of angiogenesis. We explored the distribution flow of iβ2GPI and nβ2GPI in the tumor lesion by labeling them with ^{64}Cu, creating *in vivo* PET imaging probes. This led to the discovery that iβ2GPI and nβ2GPI have similar distributions in the tumor lesions. Our findings will contribute to the further understanding of β2GPI as a potential target for the clinical treatment of angiogenesis-related diseases.

Acknowledgments. We thank Dr. Shinsuke Yasuda (Hokkaido University) and Dr. Junko Inagaki (Okayama University) for the critical discussion of this study. This research was supported by the Ministry of Education, Culture, Sports, Science and Technology of Japan KAKEN (Grant No. 26253036). ATW is the recipient of a Postgraduate Scholarship from the Directorate General of Higher Education (DGHE), Ministry of National Education of the Republic of Indonesia.

References

1. Yasuda S, Atsumi T, Ieko M and Koike T: β2-glycoprotein I, anti-β2-glycoprotein I, and fibrinolysis. Thromb Res (2004) 114: 461–465.
2. Kato H and Enjyoji K: Amino acid sequence and location of the disulfide bonds in bovine β2-glycoprotein I: the presence of five sushi domains. Biochemistry (1991) 30: 11687–11694.
3. Atsumi T, Amengual O, Yasuda S, Matsuura E and Koike T: Research around β2-glycoprotein I: a major target for antiphospholipid antibodies. Autoimmun (2005) 38: 377–381.
4. Matsuura E, Igarashi Y, Fujimoto M, Ichikawa K and Koike T: Anticardiolipin cofactor(s) and differential diagnosis of autoimmune disease. Lancet (1990) 336: 177–178.
5. Matsuura E, Igarashi Y, Fujimoto M, Ichikawa K, Suzuki T, Sumida T, Yasuda T and Koike T: Heterogenity of anticardiolipin antibodies defined by the anticardiolipin cofactor. J Immunol (1992) 148: 3885–3891.
6. Matsuura E, Igarashi Y, Yasuda T, Triplett DA and Koike T: Anticardiolipin antibodies recognize β2-glycoprotein I structure altered by interacting with an oxygen modified solid phase surface. J Exp Med (1994) 179: 457–462.
7. Matsuura E, Shen L, Matsunami Y, Quan N, Makarova M, Geske FJ, Boisen M, Yasuda S, Kobayashi K and Lopez LR: Pathophysiology of β2-glycoprotein I in antiphospholipid syndrome. Lupus (2010) 19: 379–384.
8. Ohkura N, Hagihara Y, Yoshimura T, Goto Y and Kato H: Plasmin can reduce the function of human β2-glycoprotein I by cleaving domain V into a nicked form. Blood (1998) 91: 4173–4179.
9. Hunt JE, Simpson RJ and Krilis SA: Identification of a region of β2-glycoprotein I critical for lipid binding and anti-cardiolipin antibody cofactor activity. Proc Natl Acad Sci U S A (1993) 90: 2141–2145.
10. Yasuda S, Atsumi T, Ieko M, Matsuura E, Kobayashi K, Inagaki J, Kato H, Tanaka H, Yamakado M, Akino M, Saitou H, Amasaki Y, Jodo S, Amengual O and Koike T: Nicked β2-glycoprotein I: a marker of cerebral infarct and a novel role in the negative feedback pathway of extrinsic fibrinolysis. Blood (2004) 103: 3766–3772.
11. Carmeliet P: Angiogenesis in health and disease. Nat Med (2003) 9: 653–660.
12. Ferrara N, Gerber HP and LeCouter J: The biology of VEGF and its receptors. Nat Med (2003) 6: 669–676.
13. Roskoski Jr R: Vascular Endothelial Growth Factor (VEGF) signaling in tumor progression. Hematol (2007) 62: 179–213.
14. Hoeben A, Landuyt B, Highley MS, Wildiers H, Van Oosterom AT and De Bruijn EA: Vascular endothelial growth factor and angiogenesis. Pharmacol Rev (2004) 56: 549–580.
15. Olsson AK, Dimberg A, Kreuger J and Claesson-Welsh L: VEGF receptor signaling — in control of vascular function. Nat Rev Mol Cell Biol (2006) 7: 359–371.
16. Yu P, Passam FH, Yu DM, Denyer G and Krilis SA: β2-glycoprotein I inhibits vascular endothelial growth factor and basic fibro-

blast growth factor induced angiogenesis through its amino terminal domain. J Thromb Haemost (2008) 6: 1215–1223.
17. Nakagawa H, Yasuda S, Matsuura E, Kobayashi K, Ieko M, Kataoka H, Horita T, Atsumi T and Koike T: Nicked β2-glycoprotein I binds angiostatin 4.5 (plasminogen kringle 1–5) and attenuates its antiangiogenic property. Blood (2009) 114: 2553–2559.
18. Sakai T, Balasubramanian K, Maiti S, Halder JB and Schroit AJ: Plasmin-cleaved β2-glycoprotein 1 is an inhibitor of angiogenesis. Am J Pathol (2007) 171: 1659–1669.
19. Kurdziel KA, Lindenberg L and Choyke PL: Oncologic angiogenesis imaging in the clinic—how and why. Imaging Medicine (2011) 3: 445–457.
20. Hutchins GD, Miller MA, Soon VC and Receveur T: Small animal PET imaging. ILAR J (2008) 49: 54–65.
21. Kobayashi K, Matsuura E, Liu Q, Furukawa J, Kaihara K, Inagaki J, Atsumi T, Sakairi N, Yasuda T, Voelker DR and Koike T: A specific ligand for β2-glycoprotein I mediates autoantibody-dependent uptake of oxidized low density lipoprotein by macrophages. J Lipid Res (2001) 42: 697–709.
22. Kobayashi K, Sasaki T, Takenaka F, Yakushiji H, Fujii Y, Kishi Y, Kita S, Shen L, Kumon H and Matsuura E: A novel PET imaging using ^{64}Cu-labeled monoclonal antibody against mesothelin commonly expressed on cancer cells. J Immunol Res (2015) (Article ID 268172).
23. Cooper MS, Ma MT, Sunassee K, Shaw KP, Williams JD, Paul RL, Donnelly PS and Blower PJ: Comparison of ^{64}Cu-complexing bifunctional chelators for radioimmunoconjugation: labeling efficiency, specific activity, and in vitro/in vivo stability. Bioconjug Chem (2012) 23: 1029–1039.
24. Matsuura E, Inagaki J, Kasahara H, Yamamoto D, Atsumi T, Kobayashi K, Kaihara K, Zhao D, Ichikawa K, Tsutsumi A, Yasuda T, Triplett DA and Koike T: Proteolytic cleavage of β2-glycoprotein I: reduction of antigenicity and the structural relationship. Int Immunol (2000) 12: 1183–1192.
25. Shi T, Giannakopoulos B, Iverson GM, Cockerill KA, Linnik MD and Krilis SA: Domain V of β2-glycoprotein I binds factor XI/XIa and is cleaved at Lys^{317}–Thr^{318}. J Biol Chem (2005) 280: 907–912.
26. Passam FH, Qi JC, Tanaka K, Matthaei KI and Krilis SA: In vivo modulation of angiogenesis by beta-2-glycoprotein I. J Autoimmun (2010) 35: 232–240.
27. Beecken WD, Egnl T, Ringel EM, Camphausen K, Michaelis M, Jonas D, Folkman J, Shing Y and Blaheta RA: An endogenous inhibitor of angiogenesis derived from a translational cell carcinoma: clipped beta-2-glycoprotein I. Ann Surg Oncol (2006) 13: 1241–1251.
28. Chiu Wen-Chin, Lin Jan-Yu, Lee Tzong-Shyuan, You Li-Ru and Chiang An-Na: β2-glycoprotein I inhibits VEGF-induced endothelial cell growth and migration via suppressing phosphorylation of VEGFR2, erk1/2, and akt. Mol Cell Biochem (2013) 372: 9–15.
29. Beecken WD, Ringel EM, Babica J, Opperman E, Jonas D and Blaheta RA: Plasmin-clipped β2-glycoprotein I inhibits endothelial cell growth by down-regulating cyclin a, b and d1 and up-regulating p21 and p27. Cancer Lett (2010) 296: 160–167.
30. Moriyama T, Ohuchida K, Mizumoto K, Yu J, Sato N, Nabae T, Takahata S, Toma H, Nagai E and Tanaka M: MicroRNA-21 modulates biological functions of pancreatic cancer cells including their proliferation, invasion, and chemo-resistance. Mol Cancer Ther (2009) 8: 1067–1074.
31. Zhang Y, Hong H, Engle JW, Bean J, Yang Y, Leigh BR, Barnhart TE and Cai W: Positron emission tomography imaging of CD105 expression with a ^{64}Cu-labeled monoclonal antibody: NOTA is superior to DOTA. PLoS ONE (2011) 6: e28005.
32. Caronti B, Calderaro C, Alesandri C, Conti F, Tinghino R, Palladini G and Valesini G: β2-glycoprotein I (β2-GPI) mRNA is expressed by several cell types involved in anti-phospholipid syndrome-related tissue damage. Clin Exp Immunol (1999) 115: 214–219.
33. Ma K, Simantov R, Zhang JC, Silverstein R, Hajjar KA and McCrae KR: High affinity binding of β2-glycoprotein I to human endothelial cells is mediated by annexin II. J Biol Chem (2000) 275: 15541–15548.
34. Alard JE, Gaillard F, Daridon C, Shoenfeld Y, Jamin C and Youinou P: TLR2 is one of the endothelial receptors for β2-glycoprotein I. J Immunol (2010) 185: 1550–1557.